IEEE Access
Multidisciplinary ⋮ Rapid Review ⋮ Open Access Journal

Received 22 July 2023, accepted 4 August 2023, date of publication 14 August 2023, date of current version 18 August 2023.

Digital Object Identifier 10.1109/ACCESS.2023.3304904

RESEARCH ARTICLE

Slotted Waveguide Circularly Polarized Leaky Wave Antenna With Improved Efficiency at W-Band

SHILPI SINGH, (Graduate Student Member, IEEE), SHAKTI SINGH CHAUHAN, (Member, IEEE), AND ANANJAN BASU, (Senior Member, IEEE)

Centre for Applied Research in Electronics, Indian Institute of Technology Delhi, New Delhi 110016, India

Corresponding author: Shilpi Singh (shilpi.singh@care.iitd.ac.in)

ABSTRACT This article presents a high-efficiency circularly polarized slotted waveguide leaky wave antenna for the W band frequency range. The wall thickness of the slotted waveguide leaky wave antenna containing the radiating slots is tuned to optimize the overall antenna performance. A thin dielectric layer with an array of metallic patches has been used as a linear-to-circular polarization converter. The fabrication challenges of the W band antenna have been overcome by CNC milling machines which provide a high degree of precision and accuracy. The gain of the prototype antenna is above 20 dBi in the intended operating band from 92 GHz to 98 GHz. Furthermore, the antenna provides an average half-power beamwidth (HPBW) of 3.2° in the elevation plane and a cross-polarization level below -18 dB in the main beam direction. The combination of its robust design, reliable fabrication, simple configuration, and superior performance makes the proposed antenna a strong candidate for various W band applications.

INDEX TERMS Leaky wave antenna (LWA), slotted waveguide antenna, circular polarization, W-Band, millimeter wave.

I. INTRODUCTION

The demand for larger bandwidth, higher data transfer rates, and channel capacity has increased rapidly in recent years. To meet the requirements of the future, the communication industry is shifting towards higher frequencies such as millimeter wave (mmW) frequency (30 GHz to 300 GHz) [1]. W band considered to be a frontier for space communication applications, is one of the dominant bands of mmW frequency. W-band offers an atmospheric transmission ''window'' [2] and finds application in radar imaging, security screening, non-destructive testing (NDT), etc. Due to the upcoming trends and possibilities of the W-band, the industry needs a high-performance antenna that is cost-effective and fabrication-tolerant [3], [4].

A leaky wave antenna (LWA) is an excellent candidate for mmW frequency band applications due to its inherent qualities like beam steering and high directivity. Despite the exceptional properties, only few works are available in the literature for slotted waveguide LWA. In [5], a linearly polarized slotted waveguide antenna has been presented for the W-band. A high gain slotted waveguide array antenna based on electroforming is discussed in [6]. In [7], a W band high-gain slot array antenna has been developed using a double-layer waveguide. A planar LWA for the W band is demonstrated in [8] but suffers from low radiation efficiency. Antennas reported in [6], [7], and [8] are linearly polarized, so it cannot be used for space applications. In [9] a hybrid antenna is illustrated, where to reduce transmission losses a waveguide is used in the feeding network, and an array of radiating slots was constructed on SIW.

For the W band, several SIW-based array antennas have been documented in the literature [10], [11], [12], [13], [14]. On a single PCB, a four-stage, two-way divider has been designed in [10], but its radiation efficiency is low. In [11], [12], and [13], a two-layer SIW-based antenna has

The associate editor coordinating the review of this manuscript and approving it for publication was Mohammad Zia Ur Rahman.

been developed, in which a feed network is designed on the bottom layer and another dielectric layer is added to improve the antenna gain. To reduce the loss in the W-band, multi-layer low temperature co-fired ceramics (LTCC) have been introduced in [14]. Design of SIW antenna at higher frequencies is more complicated and prone to manufacturing tolerances than at lower frequencies. The confinement of the electromagnetic field between two metallic vias is more challenging as the frequency increases.

The circularly polarized (CP) antenna is chosen over the linearly polarized antenna because it can reduce the effects of faraday rotation, suppress polarization mismatch, and mitigate multipath interference between the transmitter and the receiver [15]. Due to its extraordinarily desirable features, the W-band CP antenna has become a fascinating area of research. Several polarization conversion techniques have been reported in the literature [16], [17], [18] to achieve CP. A dielectric layer combined with radiating patches [16] and magneto-electric dipole [17] are investigated for CP. However, both are designed at low frequencies and extending these structures to the W band is quite challenging. In [18], another approach is presented for the CP antenna, in which multi-layer dielectric is used for polarization conversion. A single layer planar CP antenna has been reported in [19] for mmW operation but it has low efficiency, due to high dielectric and metallic losses. The radiation efficiency of the microstrip antenna decreases as the frequency increases because of high losses. As a result, waveguide is preferred at high frequency due to low losses.

The article [20] proposes a slotted waveguide configuration that incorporates three parasitic dipoles to enhance the axial ratio of the antenna. However, the small dimensions of the waveguide at the W band can result in coupling between the slots, which can potentially limit the antenna effectiveness in achieving the desired CP characteristics. The antenna mentioned in [21], utilizes a dual input feed to excite both horizontal and vertical components, enabling the generation of CP. In [22], a slotted waveguide with dual-mode excitation is used to achieve CP. However, due to the antenna structure and fabrication limitation, it is difficult to achieve satisfactory performance at W-band frequencies. The cross slotted waveguide array in [23] is prone to high fabrication error due to limitations in mechanical milling capabilities, which can impact the precision and accuracy of the fabricated structure. By acknowledging this issue, the article aims to present an alternative approach that mitigates these fabrication errors, resulting in improved performance and reliability.

This paper presents the development of a robust and highly efficient beam steering circularly polarized LWA designed for the W band applications. To enhance the overall radiation efficiency of the LWA, the thickness of the waveguide wall containing the radiating slots is reduced. The wall thickness of the slot is tuned to optimize the antenna performance by improving radiation characteristics. To the best of the author's knowledge, there is no prior research reported on increasing

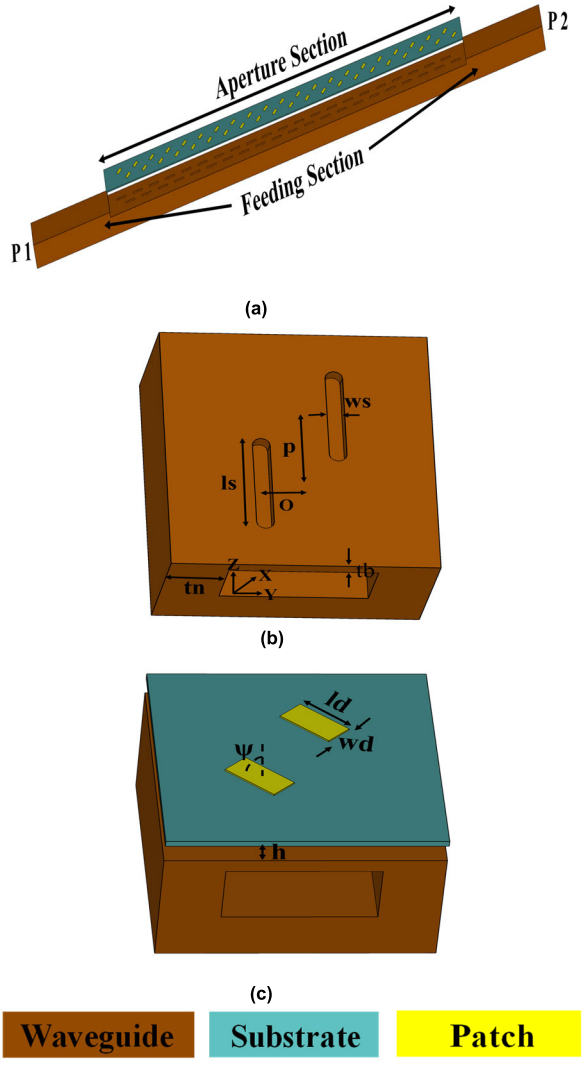

FIGURE 1. Structure details of the proposed antenna (a) Slotted waveguide antenna with polarization converter (b) Pair of longitudinal slot (c) Antenna with CP converter (ls=1.8 mm, ws=0.3 mm, o=.65 mm, p=1.6 mm, tn=1 mm, tb=0.3 mm, h=0.4 mm, ld=1.05 mm, wd=0.5 mm).

the efficiency of a slotted waveguide antenna through the reduction of slot wall thickness. The polarization converter is added to the LWA that changes the electromagnetic waves, converting the linear polarization of the incident waves into the reflected circular polarization. Furthermore, a loading effect is introduced into the structure by the integration of the polarization converter, which is providing an additional gain. The implemented antenna demonstrates excellent performance with a robust and simple antenna configuration. As a result, it is considered a strong candidate for W band applications. While a preliminary concept was previously proposed in [24], this article provides detailed information on the manufacturing process, highlighting improvements and advancements over the previous work. By describing the synthesis technique, the article provides valuable insights into the fabrication process, potentially contributing to the reproducibility and scalability of the antenna design.

II. BASIC ANTENNA CONFIGURATION AND DESIGN GUIDELINES

The properties of LWA are analyzed by designing an array of the longitudinal slot on the broad wall of the WR-10 waveguide (a = 2.54 mm, b = 1.27 mm) in a linear manner. At an offset (o) of 0.65 mm from the waveguide axis, the longitudinal slots of length (ls), width (ws), and thickness (tb) are cut. The periodicity of the slot is approximately λg/2 because the electric field inside the waveguide reverses after every λg/2 distance in the wave propagation direction, where λg is the guided wavelength of the center operating frequency. The slots are located on opposite sides of the waveguide axis, so that they all radiate in the same phase. The longitudinal slot of length 1.8 mm, and width 0.3 mm ($\approx 0.1\lambda_g$) are cut at a periodicity of 1.8 mm ($\approx 0.45\lambda_g$). Due to the high degree of sensitivity and precision required by W-band antennas, both slot ends are kept rounded.

The presented CP LWA configuration is divided into an aperture section and a feed section, as illustrated in Fig.1(a). In the aperture section, twenty-one pairs of longitudinal slots are present on the broad wall of the waveguide at an offset from the waveguide axis. While the feed section comprises a 15 mm length of WR-10 waveguide on either side of the aperture section without reducing the broad wall thickness. The WR-10 waveguide has 42 longitudinal slots and a total length of 100 mm. In order to feed the structure, a removable flange is also fabricated to connect the waveguide to the coax adapter.

A dielectric layer containing an array of metallic patches is used as a linear to circular polarization converter. The number of patches is same as the number of longitudinal slots, and it is placed just above the slotted waveguide, separated by a small air gap (h). For this structure, patches are printed on the top surface of a Rogers/ Duroid substrate ($\varepsilon_r = 2.2$, $\tan(\delta) = 0.0009$) which is 5 mil thick and positioned immediately above the radiating slots. To create a small gap between the slotted waveguide and the polarization converter, foam is placed at the corners of the polarization converter. This foam material helps to maintain the desired separation between the slots and patches. To fix the dielectric layer and foam onto the slotted waveguide, glue is used. The glue ensures that the components are firmly attached and maintain their positions during operation. A circular polarization unit consisting of a radiating slot and rotated patches on top of a dielectric layer at an angle ψ with respect to the x-axis is shown in Fig. 1(c).

In the fundamental slot theory of rectangular waveguides [25], [26] the waveguide wall thickness is negligible for calculating the resistance of radiating slot. The wall thickness of the slot will impact the performance of the radiating slot at these frequencies because the WR-10 waveguide has a 1 mm wall thickness, which is $\lambda_o/3$ at 94 GHz. The variation in S_{21} with the radiating slot thickness is seen in Fig. 2(a). From the basics, it is known that the efficiency of the antenna is directly related to the power radiated through the antenna's aperture; as a result, maximum efficiency is achieved at minimum slot thickness, as shown in Fig. 2(b).

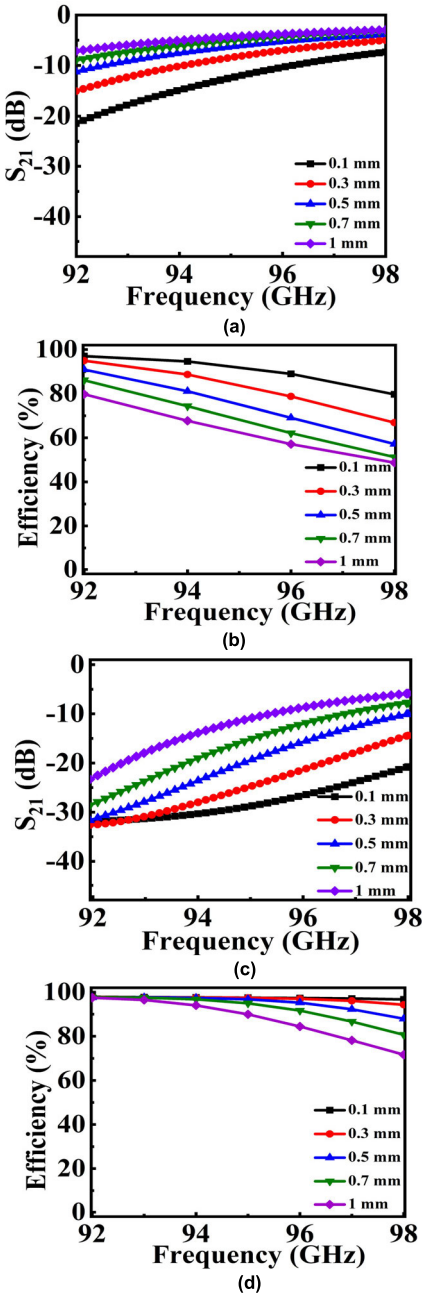

FIGURE 2. Simulated response of slotted waveguide LWA (a) S_{21} without polarization converter (b) Efficiency without polarization converter (c) S_{21} with polarization converter (d) Efficiency with polarization converter.

For CP, a polarization converter is used, which consists of metallic patches on top of the thin dielectric substrate. Due to the loading effect of the polarization converter over the slotted LWA, the overall matching of the presented antenna has improved. The increased matching has further improved S_{21} and efficiency of the presented antenna, which are illustrated in Fig. 2(c) and 2(d).

The efficiency of the proposed antenna is maximum for 0.1 mm slot thickness; longitudinal slots of this thickness would be fragile and require highly precise drill bit for

TABLE 1. Simulated gain the LWA with or without converter.

Frequency (GHz)	92	94	96	98
Gain without converter (dBi)	19.7	19.9	19.8	19.6
Gain with converter (dBi)	19.9	20.6	21.2	22.2

CNC machining. Thus for the proposed work, 0.3 mm wall thickness is chosen as its efficiency is not significantly less compared to the maximum, and slots of 0.3 mm thickness can easily be cut on the waveguide. Table 1 presents a comparison of the gain of the LWA with and without the polarization converter. The results show that the inclusion of the polarization converter has increased the realized gain of the antenna. The additional gain can be attributed to several factors associated with the antenna structure. The polarization converter has improved antenna matching, which has maximized radiated power and reduced signal reflections. Due to this, the efficiency of the antenna has increased further. The improved matching due to the presence of the polarization converter has enhanced the overall performance of the LWA.

The proposed W band circularly polarized antenna in the article offers a simple and robust design that can be fabricated using standard processes like photolithography and a Computer Numeric Control (CNC) machine. The fabrication of the antenna can be done precisely and under control using a CNC machine, resulting in repeatability and reliability. A CNC milling machine has been used only to create the slots and lower a wall thickness of the WR-10 waveguide. On the other hand, the polarization converter is fabricated using a photolithography method. The simplicity and robustness of the design, combined with the use of conventional fabrication processes, contribute to the practicality and feasibility of deploying this CP antenna in various W band applications.

Combined RHCP (E^R_{SP}) and LHCP (E^L_{SP}) radiation components from a patch (electric current) and a waveguide slot (magnetic current) is expressed as [27]:

$$E^R_{SP} = j\frac{e^{j\theta}}{\sqrt{2}} + j\sqrt{2}C_P \sin khe^{j\psi} \tag{1}$$

$$E^L_{SP} = -j\frac{e^{-j\theta}}{\sqrt{2}} + j\sqrt{2}C_P \sin khe^{-j\psi} \tag{2}$$

where

$$C_P \sin kh_{opt} = \frac{e^{j(\psi_{opt}-\theta)}}{2}\frac{\sin(\psi-\theta)}{\sin(\psi_{opt}-\theta)} \tag{3}$$

To achieve perfect circular polarization, the patch length (ld), width (wd), dielectric height (h) from the top of the waveguide surface, and patch angle (ψ) with respect to the x-axis are optimized. Solving the above equations, keeping slot angle $\theta = 0°$ with respect to the x-axis gives co-polarization and cross-polarization for arbitrary patch

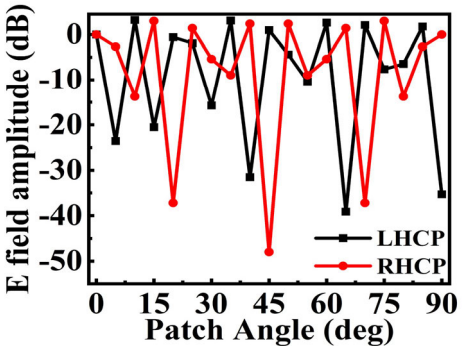

FIGURE 3. Analytical values of LHCP and RHCP at different patch angles.

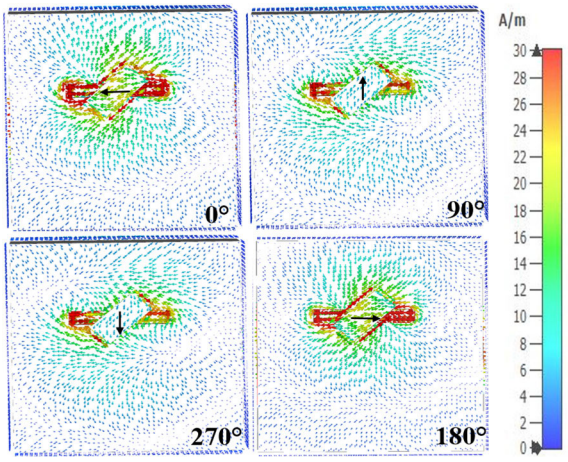

FIGURE 4. Surface current distribution at 0°, 90°,180°, 270° phase instances.

angle (ψ). For LHCP, at the designed patch angle co-polarization level (E^L_{SP}) should be maximum, and the cross-polarization level RHCP (E^R_{SP}) must be minimum, and vice versa for RHCP. Analytical expressions to determine the type of circular polarization where only the patch angle is arbitrary while other parameters are kept optimum ($\mathrm{ld} = \mathrm{ld_{opt}}$, $\mathrm{wd} = \mathrm{wd_{opt}}$ $\mathrm{h} = \mathrm{h_{opt}}$, $\psi = \psi_{\mathrm{opt}}$) is expressed as follows:

$$E^R_{SP} = \frac{je^{j\psi}}{\sin\psi_{opt}}\sin(\psi_{opt}+\psi) \tag{4}$$

$$E^L_{SP} = -\frac{je^{-j\psi}}{\sin\psi_{opt}}\sin(\psi_{opt}-\psi) \tag{5}$$

The E-field amplitude of the proposed CP antenna at the optimized patch angle is calculated from equations (4) and (5). From Fig. 3, we can say that at patch angle of 45°, the amplitude of LHCP is maximum, characterizing it as a co-polarized wave conversely RHCP is characterized as a cross-polarized wave. The sense of CP depends on the patch angle that is designed on the top surface of the substrate. By examining the direction of the surface current at different phase instances, the sense of polarization can be depicted. Based on the direction of current movement shown in Fig. 4, it is concluded that the antenna is LHCP.

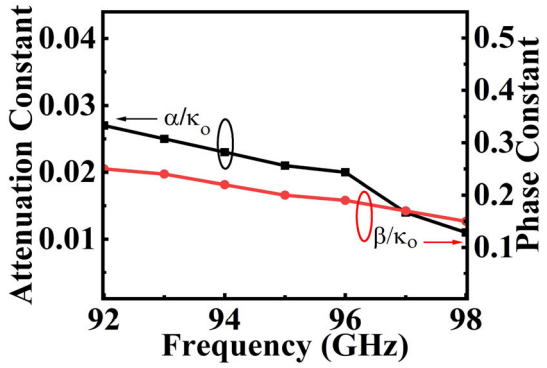

FIGURE 5. Normalized attenuation constant and phase constant of the unit cell.

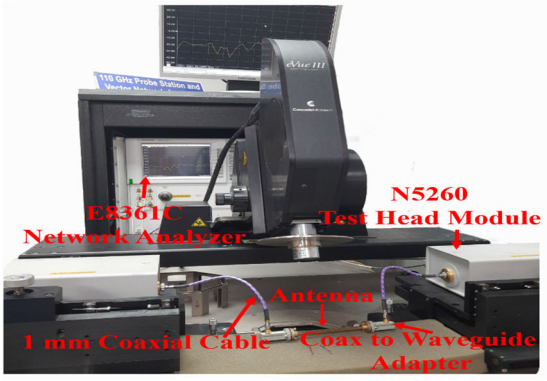

FIGURE 6. Scattering parameter measurement setup.

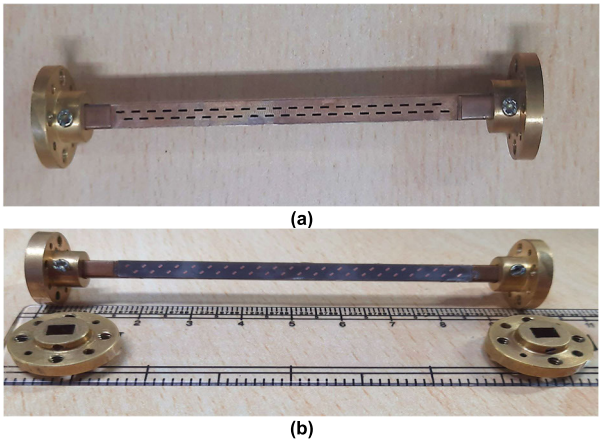

FIGURE 7. Image of fabricated antenna (a) Slotted waveguide antenna (b) Antenna with polarization converter.

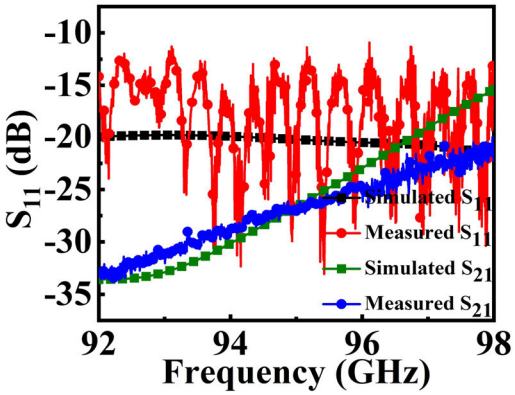

FIGURE 8. Simulated and measured scattering parameter of prototype antenna.

III. PROTOTYPE ANTENNA MEASUREMENT AND RESULT DISCUSSION

A prototype of the proposed antenna is designed, fabricated, and tested to verify the high efficiency circularly polarized antenna concept. The dispersion diagram of the proposed CP LWA in the W band is shown in Fig. 5. The value of normalized attenuation constant is close to zero, ensuring a narrow beamwidth. In the given structure normalized phase constant slope is negative, which shows that the beam is steering from endfire to broadside direction as frequency varies from 92 GHz to 98 GHz. Since $|\beta| < k_o$, the presented antenna will operate in the fast wave region for the given frequency range, where k_o is free space wavenumber. The attenuation and phase constant of the proposed LWA is calculated from the S parameter and it is expressed as follows (where p is the length of the unit cell) [28]:

$$\alpha = \frac{1}{p}\left|Re\left(\cosh^{-1}\left(\frac{1 - S_{11}S_{22} + S_{12}S_{21}}{2S_{21}}\right)\right)\right| \quad (6)$$

$$\beta = \frac{1}{p}\left|Im\left(\cosh^{-1}\left(\frac{1 - S_{11}S_{22} + S_{12}S_{21}}{2S_{21}}\right)\right)\right| \quad (7)$$

The measurement of S parameters for the proposed antenna structure was conducted using a Network Analyzer (E8361C) and an Agilent Test Module (N5360). A comparison between the simulated and measured scattering parameter of the complete antenna structure is presented in Fig. 8. The measured result shows acceptable agreement with the simulated result. Furthermore, the measured S_{11} value remains below -10 dB across the operating band, indicating a good impedance match and efficient power transfer. However, there are some discrepancies between the simulated and measured results. These discrepancies can arise due to fabrication errors or transition errors in the measurement. Since the LWA is a long structure, multiple reflections are generated from different slots due to fabrication inaccuracies, resulting in a zig zag pattern. Despite these discrepancies, the measured results still demonstrate satisfactory performance and validate the overall performance of the proposed antenna.

The 2-D normalized radiation pattern of the antenna at 92 GHz and 98 GHz are shown in Fig. 9. Beam scanning is achieved from -15° endfire to -9° broadsides direction for the 92 GHz to 98 GHz frequency respectively. This indicates that the antenna can steer its main beam over a range of angles, allowing for flexible beam positioning and coverage. The average 3 dB HPBW is 3.2° in the xz plane. The fabricated antenna exhibits side lobes below −14.5 dB throughout the operating band in the elevation

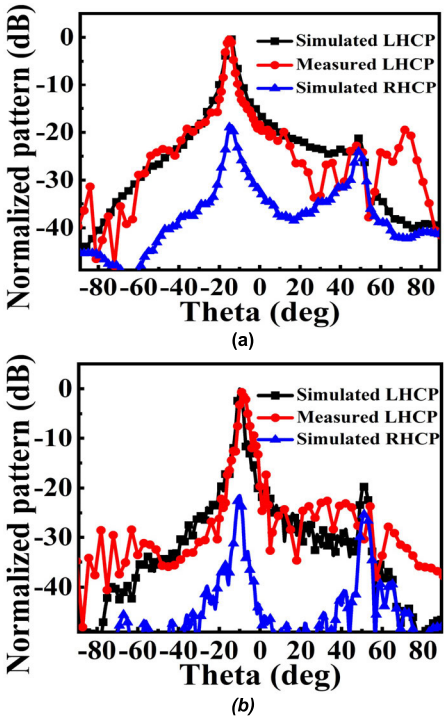

FIGURE 9. Normalized radiation pattern in elevation plane at (a) 92 GHz (b) 98 GHz.

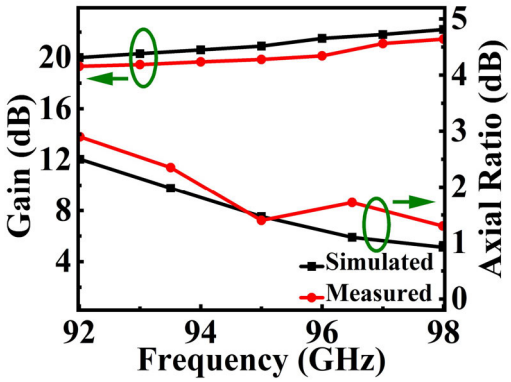

FIGURE 10. Measured and simulated: gain and axial ratio in the main beam direction.

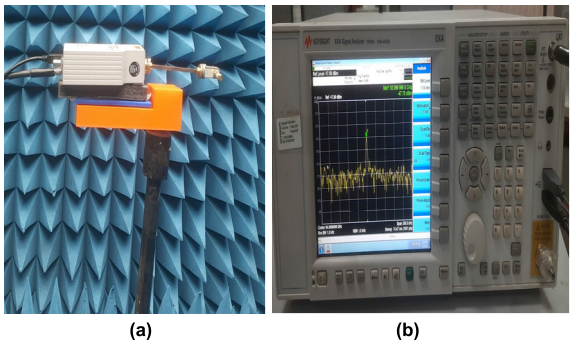

FIGURE 11. Antenna Measurement setup (a) Prototype antenna mounted on the rotating stage (b) Signal analyzer to check power level of the antenna.

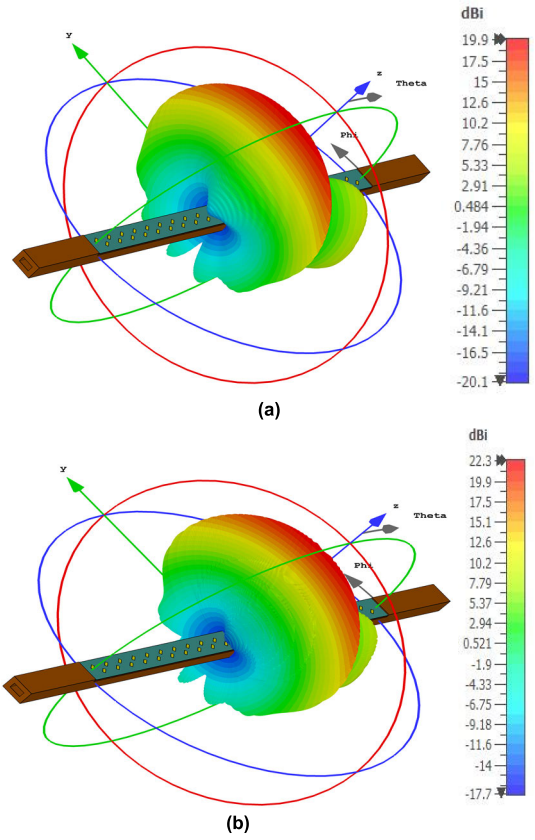

FIGURE 12. Simulated 3D radiation pattern of proposed antenna at (a) 92GHz (b) 98 GHZ.

plane. Moreover, the cross polarization level below -18 dB is realized in the main beam direction.

The comparison of gains between the simulated and measured results is highlighted in Fig. 10. The presented antenna shows almost constant gain across the entire frequency band, i.e., 92 GHz to 98 GHz. The axial ratio of the antenna, which determines the polarization purity, is reported to be below 3 dB for both ports in any feed direction. The proposed antenna exhibits a balanced and symmetrical structure, resulting in similar axial ratios for both ports throughout the operating band. The measured total efficiency of the fabricated antenna is above 76 % in the entire operating band and the maximum realized total efficiency is 82 % at 98 GHz. The gain and radiation pattern of the presented CP antenna have been measured by a linearly polarized source, and its complete procedure is described in [29]. For radiation pattern measurement, the standard WR-10 waveguide is connected to the performance network analyzer which is acting as transmitter. At the receiver side, the prototype antenna is connected to the mixer to check the received power level in the Keysight signal analyzer N9010A. The antenna is mounted on the antenna rotating stage. The received signal strength in the main beam direction is shown in Fig. 11(b). Since all the simulated results are matching

TABLE 2. Performance comparison with similar V, E, W-band antennas.

Ref.	Freq. (GHz)	Gain (dBi)	η (%)	Size (mm^2)	CP	Complexity
[6]	89.9 - 97.6	26.8	82	473 × 7.2	No	Medium
[8]	77.5 - 85.5	18	33	70 × 10	No	Medium
[9]	91.5 - 94.5	31.8	33	45 × 85	No	Medium
[10]	93 - 96	25.8	15	130 × 125	No	Medium
[13]	91 - 97	28.8	24	92 × 66	No	Low
[14]	87 - 101	23.8	42	21.6 × 21.6	No	High
[19]	85 - 86.3	23	32	80 × 75	Yes	Low
[21]	58 - 62	12	37	38 × 3.1	Yes	Medium
[23]	84 - 86	24	89	175 × 33	Yes	High
This work	92 - 98	21.4	82	100 × 4.5	Yes	Low

with the measured result and the sense of circular polarization observed from the simulator is verified analytically, so from the above findings, we can say that the presented antenna is LHCP. Furthermore, the RHCP antenna can be designed from the same proposed concept by rotating the patch at its complimentary angle. The simulated 3D radiation pattern of proposed CP LWA at 92 GHz and 98 GHz is shown in Fig. 12. It is evident from the pattern that the antenna is radiating in the broadside direction and providing a narrow beamwidth.

A comparison with recent published CP LWA is done to show that excellent antenna characteristics can also be achieved by simple structure. The paper aims to present high performance and low cost antenna for W band application. The V, E, and W band antenna designs provided in the literature and the presented W-band antenna are compared in the Table 2. The absence of a power divider in the circuit of the illustrated antenna significantly reduces the complexity of the antenna. Some antennas have higher gain than prototype antenna because of 1×4 or 1×8 array design. The proposed work has a simple structure and wide axial ratio bandwidth, as well as the efficiency is also in the acceptable limit. Broadside radiation and a narrow beamwidth are additional benefits of the proposed antenna. Furthermore, the CP attained in [22] and [23] via cross slots does not have radiation in the broadside, and the beamwidth is also broad. The presented antenna is the only 1D LWA providing gain above 20 dBi and HPBW below 4° in the elevation plane. This paper also demonstrates a cost-effective method by which a highly precise W band slotted waveguide antenna can be designed with the help of a CNC milling machine and the photolithography process. The presented antenna offers a practical and viable solution for various W-band applications where reliable and efficient communication systems are required without significant complexity or cost constraints.

IV. CONCLUSION

In this paper, a high-efficiency slotted waveguide CP LWA at the W band has been proposed. The wall thickness of a slotted waveguide LWA containing radiating slots is tuned to enhance the total radiation efficiency of the antenna. The LHCP characteristic is realized by metallic patches on a thin dielectric layer which acts as a linear to circular polarization converter. The LWA is designed using CNC milling machine while the polarization converter is fabricated by photolithography process. The proposed antenna has yielded high efficiency, broadside radiation pattern, and almost constant gain from 92 GHz to 98 GHz frequency band. Due to these extraordinary characteristics, the proposed antenna can be an excellent candidate for various W band applications.

REFERENCES

[1] A. Ghosh, T. A. Thomas, M. C. Cudak, R. Ratasuk, P. Moorut, F. W. Vook, T. S. Rappaport, G. R. MacCartney, S. Sun, and S. Nie, "Millimeter-wave enhanced local area systems: A high-data-rate approach for future wireless networks," *IEEE J. Sel. Areas Commun.*, vol. 32, no. 6, pp. 1152–1163, Jun. 2014.

[2] H. Liebe, "Atmospheric EHF window transparencies near 35, 90, 140 and 220 GHz," *IEEE Trans. Antennas Propag.*, vol. AP-31, no. 1, pp. 127–135, Jan. 1983.

[3] E. Cianca, T. Rossi, A. Yahalom, Y. Pinhasi, J. Farserotu, and C. Sacchi, "EHF for satellite communications: The new broadband frontier," *Proc. IEEE*, vol. 99, no. 11, pp. 1858–1881, Nov. 2011.

[4] T. Manabe, K. Sato, H. Masuzawa, K. Taira, K.-C. Huang, and D. J. Edwards, *Millimeter Wave Antennas for Gigabit Wireless Communications*. Chichester, U.K.: Wiley, 2008.

[5] D. A. Schneider, M. Rösch, A. Tessmann, and T. Zwick, "A low-loss W-band frequency-scanning antenna for wideband multichannel radar applications," *IEEE Antennas Wireless Propag. Lett.*, vol. 18, no. 4, pp. 806–810, Apr. 2019.

[6] D.-Y. Kim, Y. Lim, H.-S. Yoon, and S. Nam, "High-efficiency W-band electroforming slot array antenna," *IEEE Trans. Antennas Propag.*, vol. 63, no. 4, pp. 1854–1857, Apr. 2015.

[7] M. Zhang, J. Hirokawa, and M. Ando, "An E-band partially corporate feed uniform slot array with laminated quasi double-layer waveguide and virtual PMC terminations," *IEEE Trans. Antennas Propag.*, vol. 59, no. 5, pp. 1521–1527, May 2011.

[8] A. E. Olk, M. Liu, and D. A. Powell, "Printed tapered leaky-wave antennas for W-band frequencies," *IEEE Trans. Antennas Propag.*, vol. 70, no. 2, pp. 900–910, Feb. 2022.

[9] Z. Ding, S. Xiao, M.-C. Tang, and C. Liu, "A compact highly efficient hybrid antenna array for W-Band applications," *IEEE Antennas Wireless Propag. Lett.*, vol. 17, no. 8, pp. 1547–1551, Aug. 2018.

[10] Y. J. Cheng, W. Hong, and K. Wu, "94 GHz substrate integrated monopulse antenna array," *IEEE Trans. Antennas Propag.*, vol. 60, no. 1, pp. 121–129, Jan. 2012.

[11] N. Ghassemi and K. Wu, "High-efficient patch antenna array for E-band gigabyte point-to-point wireless services," *IEEE Antennas Wireless Propag. Lett.*, vol. 11, pp. 1261–1264, 2012.

[12] N. Ghassemi, K. Wu, S. Claude, X. Zhang, and J. Bornemann, "Low-cost and high-efficient W-band substrate integrated waveguide antenna array made of printed circuit board process," *IEEE Trans. Antennas Propag.*, vol. 60, no. 3, pp. 1648–1653, Mar. 2012.

[13] Y. J. Cheng, Y. X. Guo, and Z. G. Liu, "W-band large-scale high-gain planar integrated antenna array," *IEEE Trans. Antennas Propag.*, vol. 62, no. 6, pp. 3370–3373, Jun. 2014.
[14] B. Cao, H. Wang, Y. Huang, and J. Zheng, "High-gain L-probe excited substrate integrated cavity antenna array with LTCC-based gap waveguide feeding network for W-band application," *IEEE Trans. Antennas Propag.*, vol. 63, no. 12, pp. 5465–5474, Dec. 2015.
[15] C. A. Balanis, *Antenna Theory: Analysis and Design*. New York, NY, USA: Wiley, 2005.
[16] M. Asaadi and A. Sebak, "High-gain low-profile circularly polarized slotted SIW cavity antenna for MMW applications," *IEEE Antennas Wireless Propag. Lett.*, vol. 16, pp. 752–755, 2017.
[17] S. X. Ta and I. Park, "Crossed dipole loaded with magneto-electric dipole for wideband and wide-beam circularly polarized radiation," *IEEE Antennas Wireless Propag. Lett.*, vol. 14, pp. 358–361, 2015.
[18] K. X. Wang and H. Wong, "A wideband millimeter-wave circularly polarized antenna with 3-D printed polarizer," *IEEE Trans. Antennas Propag.*, vol. 65, no. 3, pp. 1038–1046, Mar. 2017.
[19] G. Mishra, S. K. Sharma, and J. S. Chieh, "A high gain series-fed circularly polarized traveling-wave antenna at W-band using a new butterfly radiating element," *IEEE Trans. Antennas Propag.*, vol. 68, no. 12, pp. 7947–7957, Dec. 2020.
[20] M. Ferrando-Rocher, J. I. Herranz-Herruzo, A. Valero-Nogueira, and V. M. Rodrigo, "Circularly polarized slotted waveguide array with improved axial ratio performance," *IEEE Trans. Antennas Propag.*, vol. 64, no. 9, pp. 4144–4148, Sep. 2016.
[21] M. García-Vigueras, E. Menargues, T. Debogovic, E. Rijk, and J. R. Mosig, "Cost-effective dual-polarised leaky-wave antennas enabled by three-dimensional printing," *IET Microw., Antennas Propag.*, vol. 11, no. 14, pp. 1985–1991, Nov. 2017.
[22] A. Dorlé, R. Gillard, E. Menargues, M. Van Der Vorst, E. De Rijk, P. Martín-Iglesias, and M. García-Vigueras, "Circularly polarized leaky-wave antenna based on a dual-mode hollow waveguide," *IEEE Trans. Antennas Propag.*, vol. 69, no. 9, pp. 6010–6015, Sep. 2021.
[23] F. N. Ayoub, Y. Tawk, E. Ardelean, J. Costantine, S. A. Lane, and C. G. Christodoulou, "Cross-slotted waveguide array with dual circularly polarized radiation at W-band," *IEEE Trans. Antennas Propag.*, vol. 70, no. 1, pp. 268–277, Jan. 2022.
[24] S. Singh and A. Basu, "Circularly polarized slotted waveguide leaky wave antenna at W band for radar application," in *Proc. Int. Symp. Antennas Propag. (ISAP)*, Oct. 2022, pp. 403–404.
[25] A. F. Stevenson, "Theory of slots in rectangular wave-guides," *J. Appl. Phys.*, vol. 19, no. 1, pp. 24–38, Jan. 1948.
[26] R. Hyneman, "Closely-spaced transverse slots in rectangular waveguide," *IRE Trans. Antennas Propag.*, vol. 7, no. 4, pp. 335–342, Oct. 1959.
[27] K.-S. Min, J. Hirokawa, K. Sakurai, and M. Ando, "Phase control of circularly polarized waves from a parasitic dipole mounted above a slot," in *Proc. IEEE Antennas Propag. Soc. Int. Symp.*, Feb. 1997, pp. 1348–1351.
[28] N. Javanbakht, M. S. Majedi, and A. R. Attari, "Thinned array inspired quasi-uniform leaky-wave antenna with low side-lobe level," *IEEE Antennas Wireless Propag. Lett.*, vol. 16, pp. 2992–2995, 2017.
[29] B. Yen Toh, R. Cahill, and V. F. Fusco, "Understanding and measuring circular polarization," *IEEE Trans. Educ.*, vol. 46, no. 3, pp. 313–318, Aug. 2003.

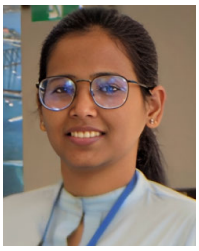

SHILPI SINGH (Graduate Student Member, IEEE) received the B.Tech. degree in electronics and communication from the Krishna Engineering College Ghaziabad, and the M.Tech. degree in RF and microwave engineering from the Indian Institute of Information Technology, Design and Manufacturing, Jabalpur, India. She is currently pursuing the Ph.D. degree with the Indian Institute of Technology Delhi (IIT Delhi), Delhi, India. Her research interests include leaky wave antenna, slotted waveguide antenna, sub terahertz imaging, millimeter wave RF components, and reconfigurable antennas. She has served as the Chairperson and the Treasurer of IEEE MTT-S Student Branch Chapter IIT Delhi.

SHAKTI SINGH CHAUHAN (Member, IEEE) received the B.Tech. degree from UKTU, Dehradun, in 2010, and the master's degree in electronics and communication, in 2012. He is currently pursuing the Ph.D. degree with the Indian Institute of Technology Delhi, Delhi, India. He was a Faculty Member of the ECE Department, BIAS, Bhimtal, from August 2012 to December, 2014. His current research interest includes millimeterwave antennas. He was a recipient of the Visvesverya Fellowship from the Ministry of Electronics and IT, New Delhi, India.

ANANJAN BASU (Senior Member, IEEE) received the B.Tech. degree in electrical engineering and the M.Tech. degree in communication and radar engineering from the Indian Institute of Technology Delhi (IIT Delhi), in 1991 and 1993, respectively, and the Ph.D. degree in electrical engineering from the University of California at Los Angeles (UCLA), in 1998. He was with the Centre for Applied Research in Electronics, IIT Delhi, as an Assistant Professor, from 2000 to 2005, and an Associate Professor, from 2005 to 2012, where he has been a Professor, since 2013. His research interests include microwave and millimeter-wave component design and characterization.